

# Characterization of Geiger-Müller radiation detectors response at the University of Costa Rica's Cyclotron Facilities

Caracterización de la respuesta de detectores de radiación Geiger-Müller en el  
Ciclotrón de la Universidad de Costa Rica

Sebastián Herrera-Sánchez<sup>1</sup>, Ernesto Corrales-Corrales<sup>2</sup>, Gerardo Noguera-Vega<sup>2</sup> & Erick Mora-Ramírez<sup>2</sup>

---

**HERRERA-SANCHEZ, S.; CORRALES-CORRALES, E.; NOGUERA-VEGA, G. & MORA-RAMIREZ, E.** Characterization of Geiger-Müller radiation detectors response at the University of Costa Rica's Cyclotron Facilities. *J. health med. sci.*, 7(4):231-238, 2021.

**ABSTRACT:** To ensure a reliable verification of a radiation detector, the right parameters for this response verification must be determined and a specific characterization on the detectors of interest must be performed. These were the main pillars of this study, where four Geiger-Müller at the University of Costa Rica's Cyclotron Facilities' main laboratories were studied and characterized using a <sup>137</sup>Cs source. First, a verification of the inverse-square law was performed to corroborate the correct measurement by the detectors as the distance from a <sup>137</sup>Cs source to the detectors was varied using a new design for a positioner support to ensure repeatability. This verification yielded a potential fit curve with and equation  $D=670635 x^{-1.961}$  (error percentage of 1.95%) and an R<sup>2</sup> value of 0.9836. Then, using combinations of copper plates of widths 1.0 mm and 2.0 mm as attenuators between the source and the detectors, the mass attenuation coefficient for copper was obtained only as a reference value for future calibrations of the detectors. The result for this value was 0.040 cm<sup>2</sup>/g. The results obtained in this study and the method developed to achieve these results will serve as a base for calibrations of the detectors at these facilities, which will ensure the safety of the patients and personnel in this building.

**PALABRAS CLAVES:** Cesium 137, Geiger Müller, inverse-square law, mass attenuation coefficient, metrologic calibration, radiation detector, inverse-square law.

---

## INTRODUCTION

Thomson (1896) first described the ionization of air molecules due to their interaction with X-rays shortly after their discovery by Röntgen in 1895. This phenomenon was then used by Rutherford and the Curies for their respected work about radioactivity and radiation particles.

Radiations from a radioactive material transfer energy to atoms and molecules of a stable material when they pass through them. These interactions can either excite the atom or molecule or ionize it. When the irradiated material is part of a living being, the energy transfer can be of great danger, scaling up from a molecular level all the way to threatening the life of the being (Cherry *et al.*, 2012). Therefore, a great concern has risen since the early work previously mentioned was performed on radioactive material, with a great necessity

of being able to measure and quantify the amount of radiation a human being can be exposed to. Moreover, since the first nuclear reactors were constructed the detection for ionizing radiation has also been a "key factor in public concern" (Pandey *et al.*, 2017).

In light of this necessity, radiation detectors like the Geiger-Müller counter have been used for many years in order to ensure the safety of people working around areas with a high radiation exposure risk. It is named after Hans Geiger, who developed the theory and the concept for this type of detector in 1908, and Walther Müller, who collaborated with Geiger to develop the technique necessary to accomplish the full development of detector that could quantify various types of radiation in a practical compact tube (Pandey *et al.*, 2017).

<sup>1</sup>Escuela de Física, Universidad de Costa Rica; San José, Costa Rica.

<sup>2</sup>Centro de Investigación en Ciencias Atómicas, Nucleares y Moleculares (CICANUM), Universidad de Costa Rica; San José, Costa Rica.

In March of 2020 the first cyclotron in Costa Rica was installed in the facilities that the University of Costa Rica (UCR) destined for this project. Along with the cyclotron, six individual Geiger-Müller (GM) and sodium iodide (NaI) radiation detectors were installed in different spaces of the UCR's Cyclotron facilities as the environmental radiation monitoring system. This system is crucial ensure the safety in the working area.

In this work, only the main four GM detectors will be studied. These detectors were labeled as SA1, SA2, SA3 and SA4, located in the Quality Control Laboratory, Research Synthesis Laboratory, Packaging Room and Clinical Synthesis Laboratory respectively.

Due to the national regulations regarding the control over ionizing radiation, a periodic calibration of these detectors must be conducted; the calibrations can be performed every 1-2 years, depending on the type of detector and the Costa Rica's Ministry of Health's regulations.

Fortunately, the University of Costa Rica's Atomic, Nuclear and Molecular Science Research Center (CICANUM) has the technical capabilities to perform the corresponding calibrations, thanks to the Ionizing Radiation Metrologic Laboratory (LMRI); therefore, this process can be done without incurring in expensive and complicated procedures abroad. Hence, a study must be done in order to determine the optimal parameters that will be used in the subsequent calibrations.

Therefore, the aim of this study is to characterize the response of the main four GM environmental detectors installed in the production area of the UCR's Cyclotron Facilities.

## MATERIALS AND METHOD

To complete the objectives of this study, one of the four Geiger-Müller was analyzed and characterized. In order to do so, the response of the detectors for the activity of a  $^{137}\text{Cs}$  source was registered for a varying distance from the source to the detector. This method was performed on four different detectors located at the Cyclotron facilities denoted as SA1, SA2, SA3 and SA4. These are respectively located in the Quality Control Laboratory,

the Synthesis Laboratory for Research, the Packaging Room and the Clinical Synthesis Laboratory. This was achieved through the following objectives:

1. Verify the inverse square behavior of the radiation detected with the variation of distance from the source to the detector.
2. Obtain a reliable set of data that will serve as the base of future metrological confirmations and characterizations of the Geiger-Müller environmental detectors available at the UCR's Cyclotron Facilities.
3. Calculate the mass attenuation coefficient for copper for five distances from the source to the detector using a  $^{137}\text{Cs}$  radioactive source. The steps of this method are detailed in the following subsections.

### a. $^{137}\text{Cs}$ as a radiation source

To maintain a stable decay rate throughout the entire characterization process, this source needs to have a very long half-life period compared



Fig. 1.  $^{137}\text{Cs}$  radioactive source used to perform all of the measurements for the characterization done in this study inside its lead case.

to the time span needed to complete such measurements and reading of the detector. A cesium 137 ( $^{137}\text{Cs}$ ) source was used. The gamma rays produced by this source have an energy of 662 keV and its half-life is 30.1 years. (Parsons, 2012). All measurements were performed using a  $^{137}\text{Cs}$  source by Eckert & Ziegler Isotope Products, with a reported activity of 250.7  $\mu\text{Ci}$  dated on December 1st, 2019. The details of the source are shown in Figure 1.

### b. Experiment assembly

To ensure the repeatability and standardization of the experiment, the setup shown in Figure 2 was implemented. This assembly design allows the optimal alignment of the source with the detector. It also allows the horizontal displacement in steps of 7.5 mm, which will be used to study the relation between the radiation exposure response of the detector and the distance from the source to the detector. Moreover, the source's case has a gap that fits the copper sheets of widths ranging from 1.0 mm to 7.0 mm to measure the attenuation effect of this metal in the radiation measurement.

### c. Absolute distance measurement

The method used to accurately determine the distance from the source to the detector is better explained using Figure 3.

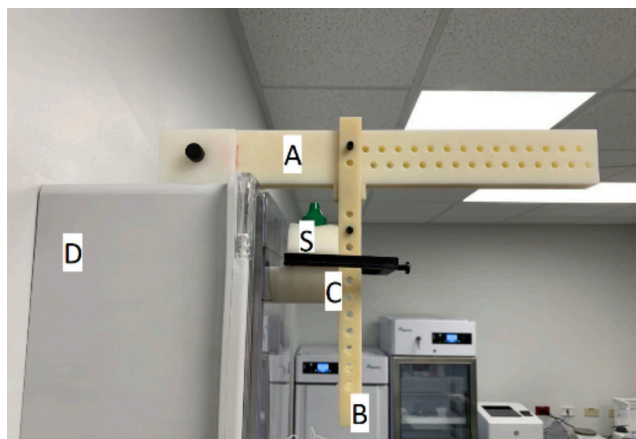


Fig. 2. Source positioner support developed by the UCR's Atomic, Nuclear and Molecular Science Research Center's personnel (own design) used to measure the radiation exposure at a varying distance of the source to the detector, where "A" is the horizontal mast that allows the horizontal displacement of the source, "B" is the vertical post that allows the vertical alignment of the source and the detector, "C" is the source's case, "D" is the detector case mounted into the wall and "S" is the radioactive source.



Fig. 3. Display of the Geiger-Müller sensor located outside its respective room showing the current reading of radiation exposure.

Using the distance sub-measurements shown in this figure, the distance required for this experiment was calculated using the following equation.

$$D = x_1 + x_2 + x_3 - x_4$$

All these measurements were performed using a digital caliper with an accuracy of 0.01 mm.

### d. Radiation exposure response measurement

Once a specific distance is set, the GM detector shows its measurement in the display that is shown in Figure 4 in units of  $\mu\text{Sv/hr}$ . Moreover, the reading of the detector is registered by the Ludlum Universal software every two seconds along with its corresponding timestamp.

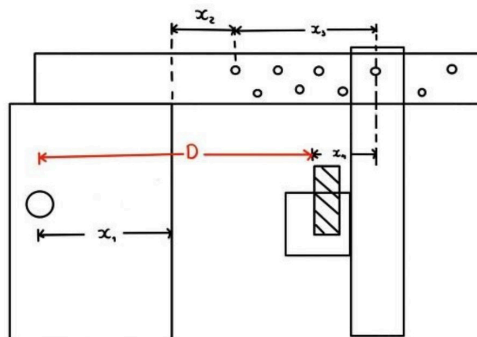


Fig. 4. Experimental method used to determine the distance from the source to the detector, where  $x_1$  is the distance from the detector to the outer wall of its case,  $x_2$  is the distance from the outer wall to the first horizontal position available in the horizontal mast,  $x_3$  is the variable distance,  $x_4$  is the distance from the center of the vertical post to the edge of the source that is closest to the detector and  $D$  is the total distance of the source to the detector (Own design).

This reading, however, shows a considerable instability. Therefore, the source stays in that same position for  $\approx 30$  seconds for the detector reading to stabilize. Then, the initial timestamp is registered in a spreadsheet for that specific position. Next, the source stays there for another 90 seconds; the readings on these 90 seconds are the ones relevant to the measurements and calculations made on this study. Finally, the readings are extracted from the Ludlum Universal software as a CSV file and the reading within the registered timestamps were averaged to obtain the average radiation dose at that specific distance. The final data analysis explained in section V performed using Microsoft Office Excel.

Finally, a new distance is set and the steps described in this section were performed over again for a total of 20 values of the distance  $x_3$  (see Figure 3).

### e. Determination of the mass attenuation coefficient

Once a relation between distance and radiation dose has been established from section IV.c, the source was placed at approximately 210-220 mm from the detector. Using a similar method, combinations of copper plates of widths equal to 1.0 mm 2.0 mm were placed in front of the source, with a total copper width ranging from 0 to 7.0 mm. The combinations used were:

- Copper width 1.0 mm: One 1.0 mm plate.
- Copper width 2.0 mm: One 2.0 mm plate.
- Copper width 3.0 mm: One 1.0 mm plate and one 2.0 mm plate.
- Copper width 4.0 mm: Two 2.0 mm plates.
- Copper width 5mm: One 1.0 mm plate and two 2.0 mm plates.
- Copper width 6.0 mm: Two 1.0 mm plates and two 2 mm plates.
- Copper width 7.0 mm: Three 1 mm plates and two 2 mm plates.

For each width, one the copper plate is placed, 30 seconds elapsed while the reading stabilizes. Then, the initial timestamp was registered and another 90 seconds elapsed. Finally, the readings were extracted from the Ludlum Universal software as a CSV file and processed accordingly using Microsoft Office Excel.

## RESULTS

### a. Verification of the inverse-square law

When implementing the method described in section IV for all four GM detectors at the Cyclotron Facilities with no attenuation material, the data detailed in Table I was obtained. The relationship between the radiation dose detected and the distance between the source and the detector is better visualized with the plot displayed in Figure 5.

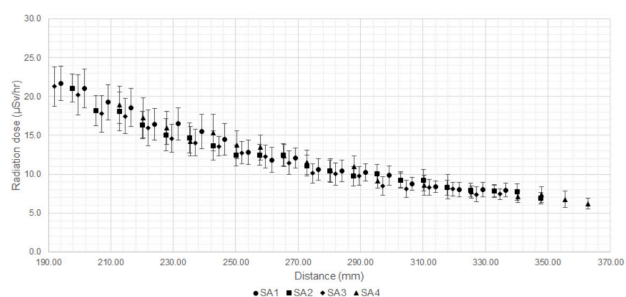


Fig. 5. Average radiation dose detected in  $\mu\text{Sv/hr}$  as a function of the absolute distance from the source to the detectors for each of the detectors.

### b. Determination of the mass attenuation coefficient

For this section of this study, the data obtained for each detector is shown in Table II.

Figures 6, 7, 8 and 9 display the respective plots for the data obtained.

After performing an exponential curve fit to determine the linear attenuation coefficient of co-

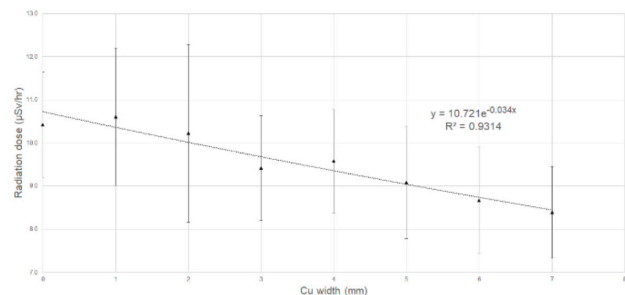


Fig. 6. Average radiation dose detected in  $\mu\text{Sv/hr}$  as a function of the total width of the copper plates placed between the source and the detector to determine the mass attenuation coefficient of detector SA1 at the UCR's Cyclotron Facilities.

pper in each specific setup from the resulting exponent and calculating the mass attenuation coefficient for each case, the results in Table III were obtained.

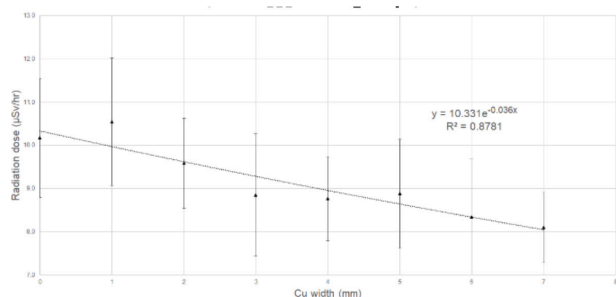


Fig. 7. Average radiation dose detected in  $\mu\text{Sv/hr}$  as a function of the total width of the copper plates placed between the source and the detector to determine the mass attenuation coefficient of detector SA2 at the UCR's Cyclotron Facilities.

## DISCUSSION

### a. Verification of the inverse-square law

Notice that this data should follow the inverse-square law because it is gamma radiation. When performing a potential fit to these data points, the

Table I. Data obtained for each GM detector at the UCR's Cyclotron Facilities for the verification of the inverse-square behavior of the gamma radiation dose detected with the variation of the distance between the source and the detector.

SA1			SA2			SA3			SA4		
Distance (mm)	Average ( $\mu\text{Sv/hr}$ )	St. Dev. ( $\mu\text{Sv/hr}$ )	Distance (mm)	Average ( $\mu\text{Sv/hr}$ )	St. Dev. ( $\mu\text{Sv/hr}$ )	Distance (mm)	Average ( $\mu\text{Sv/hr}$ )	St. Dev. ( $\mu\text{Sv/hr}$ )	Distance (mm)	Average ( $\mu\text{Sv/hr}$ )	St. Dev. ( $\mu\text{Sv/hr}$ )
186.54	24.5	2.3	197.71	21.1	1.8	184.52	23.5	2.2	212.88	18.9	2.4
194.04	21.7	2.2	205.21	18.2	2.0	192.02	21.3	2.5	220.38	17.3	2.6
201.54	21.0	2.5	212.71	18.1	2.5	199.52	20.2	2.6	227.88	16.0	2.1
209.04	19.3	2.3	220.21	16.4	1.8	207.02	17.8	2.4	235.38	14.2	1.9
216.54	18.5	2.4	227.71	15.1	2.1	214.52	17.5	2.2	242.88	15.4	2.4
224.04	16.5	2.0	235.21	14.7	2.0	222.02	16.0	2.3	250.38	13.8	1.8
231.54	16.5	2.1	242.71	13.7	1.9	229.52	14.6	1.8	257.88	13.4	1.6
239.04	15.5	2.2	250.21	12.4	1.3	237.02	14.1	1.7	265.38	12.4	1.4
246.54	14.5	2.0	257.71	12.5	1.3	244.52	13.6	1.2	272.88	11.5	1.6
254.04	12.9	1.6	265.21	12.5	1.5	252.02	12.8	1.4	280.38	10.5	1.5
261.54	11.8	1.6	272.71	11.1	1.4	259.52	12.3	1.5	287.88	11.0	1.4
269.04	12.1	1.3	280.21	10.4	1.4	267.02	11.5	1.5	295.38	9.2	1.0
276.54	10.6	1.4	287.71	9.8	1.3	274.52	10.1	1.2	302.88	9.3	1.1
284.04	10.4	1.4	295.21	10.0	1.2	282.02	10.0	1.4	310.38	8.6	1.3
291.54	10.2	1.1	302.71	9.3	0.9	289.52	9.8	1.2	317.88	8.4	1.5
299.04	9.8	1.2	310.21	9.2	1.4	297.02	8.5	1.2	325.38	7.7	0.8
306.54	8.7	0.8	317.71	8.3	1.0	304.52	8.2	1.1	332.88	7.9	0.8
314.04	8.4	0.7	325.21	8.0	0.8	312.02	8.3	1.0	340.38	7.1	0.8
321.54	8.0	0.9	332.71	7.8	0.8	319.52	8.1	0.9	347.88	7.4	1.0
329.04	8.0	0.9	340.21	7.7	1.1	327.02	7.4	0.9	355.38	6.8	1.0
336.54	8.0	0.9	347.71	6.9	0.8	334.52	7.4	0.7	362.88	6.2	0.7

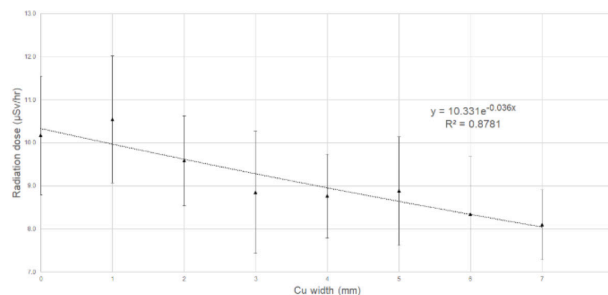


Fig. 8. Average radiation dose detected in  $\mu\text{Sv/hr}$  as a function of the total width of the copper plates placed between the source and the detector to determine the mass attenuation coefficient of detector SA3 at the UCR's Cyclotron Facilities.

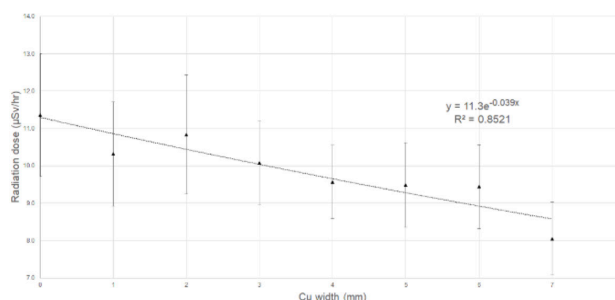


Fig. 9. Average radiation dose detected in  $\mu\text{Sv/hr}$  as a function of the total width of the copper plates placed between the source and the detector to determine the mass attenuation coefficient of detector SA4 at the UCR's Cyclotron Facilities.

Table II. Data obtained for each GM detector UCR's Cyclotron Facilities for the determination of the mass attenuation coefficient through the study of the relationship between the radiation dose detected as a function of the copper attenuator's width.

SA1			SA2			SA3			SA4		
Abs. Distance: 276.54 mm			Abs. Distance: 272.71 mm			Abs. Distance: 274.52			Abs. Distance: 212.88 mm		
Cu Width (mm)	Average (µSv/hr)	St. Dev. (µSv/hr)	Cu Width (mm)	Average (µSv/hr)	St. Dev. (µSv/hr)	Cu Width (mm)	Average (µSv/hr)	St. Dev. (µSv/hr)	Cu Width (mm)	Average (µSv/hr)	St. Dev. (µSv/hr)
0	10.4	1.2	0	11.3	1.1	0	10.2	1.4	0	11.4	1.6
1	10.6	1.6	1	11.1	1.4	1	10.5	1.5	1	10.3	1.4
2	10.2	2.1	2	10.7	1.4	2	9.6	1.0	2	10.8	1.6
3	9.4	1.2	3	10.5	1.7	3	8.8	1.4	3	10.1	1.1
4	9.6	1.2	4	10.3	1.3	4	8.8	1.0	4	9.6	1.0
5	9.1	1.3	5	9.1	1.2	5	8.9	1.3	5	9.5	1.1
6	8.7	1.2	6	9.6	1.4	6	8.3	1.3	6	9.4	1.1
7	8.4	1.1	7	8.7	0.0	7	8.1	0.8	7	8.0	1.0

Table III. Results obtained for the determination of the linear and mass attenuation coefficients for copper on the specific setups used in every GM detector studied at the UCR's Cyclotron Facilities.

	Equation	Linear	Mass
SA1	$D = 10.72e^{-0.034x}$	0.340	0.038
SA2	$D = 11.51e^{-0.036x}$	0.360	0.040
SA3	$D = 10.33e^{-0.036x}$	0.360	0.040
SA4	$D = 11.30e^{-0.039x}$	0.390	0.044

equation obtained for the relationship between the detected dose D and the distance from the source to the detector x is  $D=670635 x^{-1.961}$  with an R<sup>2</sup> value of 0.9836. This result yielded an error percentage of only 1.95%.

The reason for the non-perfect inverse-square fit of that is that the isotropic nature of the radiation and factors like the presence of metallic materials reflecting gamma rays were affecting the radiation dose detected, causing an oscillation of the data. This effect is more prominent for smaller distances, as it is showed from the error bars in Figure 5. As the source gets farther from the detector, the radiation dose intensity becomes more stable; this translates into a smaller standard deviation for the collected data.

The reason for the non-perfect inverse-square fit of that is that the isotropic nature of the radiation and factors like the presence of me-

tallic materials reflecting gamma rays were affecting the radiation dose detected, causing an oscillation of the data. This effect is more prominent for smaller distances, as it is showed from the error bars in figure VII. As the source gets farther from the detector, the radiation dose intensity becomes more stable; this translates into a smaller standard deviation for the collected data.

### b. Determination of the mass attenuation coefficient

From equation 3, the mass attenuation coefficient depends on the density of the material. In this case, the attenuating material was copper, which has a reported density of 8.94 g/cm<sup>2</sup>. (National Center for Biotechnology, n. d.). This was the density value used for our calculations.

According to Seltzer (1995), the mass attenuation coefficient of copper for an incident radiation energy of 0.6 MeV is 0.07625 cm<sup>2</sup>/g and for a radiation energy of 0.8 MeV the coefficient is 0.06605 cm<sup>2</sup>/g. Interpolating for 0.662 MeV, the mass attenuation coefficient is 0,0731 cm<sup>2</sup>/g. Compared to this reference point, our results for each detector presents a 48.08%, 45.34%, 45.34% and 39.86% of error.

Other sources of error are: first, the attenuation phenomenon occurs for a narrow-beam geometry (Cherry *et al.*, 2012), where the incident gamma rays are directly pointed at the collimated detector in a collimated beam. Then, geometry of our experiment relies on a broad-beam geometry instead. Second, all detectors were positioned within a plas-

tic box to avoid any damage; however, these boxes are made from different manufactures, then scatter may be different. Third, two detectors were placed close to concrete walls or hot cells; therefore, scatter from these structures may have had an impact on the measurements. Knowing these differences an important result is that all mass attenuation coefficients are very similar and in the same order of magnitude.

## CONCLUSION

An efficient method was successfully developed for the reliable characterization of the response of the GM detector at the UCR's Cyclotron Facilities.

A clear inverse-square relationship was observed between the radiation dose detected when the distance between the source and the detector is varied, which was expected from a  $^{137}\text{Cs}$  source that decays into gamma rays.

The obtained values for the mass attenuation coefficients vary according to reported values, these results, as well as the relationship shown in figure VII and data from Table 1, serve as a reliable data set to be used in the future for subsequent metrological verifications at the UCR's Cyclotron's GM detectors.

Uncertainty analysis will be performed in the future. Moreover, to further study the mass attenuation coefficient, a new experiment assembly will be developed to ensure a narrow-beam geometry that allows the correct analysis of the attenuation phenomenon.

---

**HERRERA-SÁNCHEZ, S.; CORRALES-CORRALES, E.; NOGUERA-VEGA, G. & MORA-RAMÍREZ, E.** Caracterización de la respuesta de detectores de radiación Geiger-Müller en el Ciclotrón de la Universidad de Costa Rica. *J. health med. sci.*, 7(4):231-238, 2021.

**RESUMEN:** Para asegurar respuesta correcta de un detector de radiación, se deben determinar los parámetros correctos para esta verificación y debe realizarse una caracterización específica de los detectores de interés. Estos fueron los pilares principales de este estudio, donde se estudiaron y caracterizaron 4 detectores Geiger-Müller en los laboratorios principales del Ciclotrón de la Universidad de Costa Rica utilizando una fuente radiactiva de  $^{137}\text{Cs}$ . Primero, se realizó una verificación

de la ley del inverso-cuadrado para corroborar la medición correcta de los detectores según se varía la distancia entre la fuente de  $^{137}\text{Cs}$  al detector utilizando un diseño nuevo de un soporte posicionador para la fuente que asegura la repetibilidad entre experimentos. Esta verificación resultó en una curva de ajuste potencial de ecuación  $D=670635x-1,961$  (porcentaje de error de 1,95%) y un valor de  $R^2$  de 0,9836. Luego, utilizando combinaciones de placas de cobre de espesores 1,0 mm y 2,0 mm como atenuadores entre la fuente y los detectores, se obtuvo el coeficiente de atenuación másico para el cobre como un valor de referencia para futuras calibraciones de los detectores. Este resultado fue de 0,040  $\text{cm}^2/\text{g}$ . Los resultados obtenidos en esta investigación y el método desarrollado para lograr estos resultados servirán como una base para una futura confirmación metroológica calibraciones de los detectores en estos laboratorios, lo cual colaborará con la seguridad y protección radiológica de pacientes y trabajadores en este edificio.

**PALABRAS CLAVES:** Calibración metroológica, Cesio 137, coeficiente de atenuación másico, Geiger Müller, ley del inverso cuadrado.

## REFERENCES

- Alpen, E. L. (1998). Energy Transfer Processes. En Radiation Biophysics (pp. 78-103). Elsevier. <https://doi.org/10.1016/B978-012053085-4/50007-7>
- Cherry, S. R., Phelps, M. E., & Sorenson, J. A. (2012). Physics in Nuclear Medicine (4.a ed.). Saunders Elsevier.
- Hussein, E. M. A. (2007). Cross Sections. En Radiation Mechanics (pp. 153-245). Elsevier. <https://doi.org/10.1016/B978-008045053-7/50004-5>
- Maruyama, R. (2021). Phenomenology of Gamma Ray and Charged Particles Interactions. En Encyclopedia of Nuclear Energy (pp. 117-124). Elsevier. <https://doi.org/10.1016/B978-0-12-819725-7.00127-6>
- McParland, B. J. (2010). Nuclear Medicine Radiation Dosimetry. Springer London. <https://doi.org/10.1007/978-1-84882-126-2>
- Pandey, S., Pandey, A., Deshmukh, M., & Shrivastava, A. K. (2017). Role of Geiger Muller Counter in Modern Physics. 7(5), 192-196.
- Parsons, B. J. (2012). Sterilisation of healthcare products by ionising radiation: Principles and standards. En Sterilisation of Biomaterials and Medical Devices (pp. 56-70). Elsevier. <https://doi.org/10.1533/9780857096265.56>
- Peruoco, R. (2014). Plain Radiographic Imaging. En Clinical Imaging (pp. 1-43). Elsevier. <https://doi.org/10.1016/B978-0-323-08495-6.00001-4>
- Schäfers, K. P., Bolwin, K., Büther, F., Hermann, S., Jacobs, A. H., Kösters, T., Kuhlmann, M., Schäfers, M., & Viel, T. (2014). High-Resolution Small Animal Imaging. En Comprehensive Biomedical Physics (pp. 181-211). Elsevier. <https://doi.org/10.1016/B978-0-444-53632-7.00110-6>

- Seltzer, S. (1995). Tables of X-Ray Mass Attenuation Coefficients and Mass Energy-Absorption Coefficients, NIST Standard Reference Database 126 [Data set]. National Institute of Standards and Technology. <https://doi.org/10.18434/T4D01F>
- Thomson, J. J. (1896). The Röntgen Rays. *Nature*, 53(1374), 391-392. <https://doi.org/10.1038/053391c0>
- Verhey, L. J., & Petti, P. L. (2010). Principles of Radiation Physics. En Leibel and Phillips Textbook of Radiation Oncology (pp. 95-119). Elsevier. <https://doi.org/10.1016/B978-1-4160-5897-7.00007-X>

Dirección para correspondencia:  
Erick Mora-Ramírez  
Escuela de Física,  
Universidad de Costa Rica;  
San José  
COSTA RICA

Email: [erick.mora@ucr.ac.cr](mailto:erick.mora@ucr.ac.cr)

Recibido: 21-06-2021

Aceptado: 07-10-2021